energies

MDPI

Article

Ground-State Redox Potentials Calculations of D-π-A and D-A-π-A Organic Dyes for DSSC and Visible-Light-Driven Hydrogen Production

Sanaz Mohammadpourasl [1], Fabrizia Fabrizi de Biani [2], Carmen Coppola [1,3], Maria Laura Parisi [1,3,4], Lorenzo Zani [4], Alessio Dessì [4], Massimo Calamante [4], Gianna Reginato [4], Riccardo Basosi [1,3,4] and Adalgisa Sinicropi [1,3,4,*]

1 R^{2}ES Lab, Department of Biotechnology, Chemistry and Pharmacy, University of Siena, 53100 Siena, Italy; sanaz.mohammadpourasl@unifi.it (S.M.); carmen.coppola@student.unisi.it (C.C.); marialaura.parisi@unisi.it (M.L.P.); riccardo.basosi@unisi.it (R.B.)
2 Department of Biotechnology, Chemistry and Pharmacy, University of Siena, 53100 Siena, Italy; fabrizia.fabrizi@unisi.it
3 Center for Colloid and Surface Science (CSGI), 50019 Sesto Fiorentino, Italy
4 National Research Council, Institute for the Chemistry of OrganoMetallic Compounds (CNR-ICCOM), 50019 Sesto Fiorentino, Italy; lorenzo.zani@iccom.cnr.it (L.Z.); a.dessi@iccom.cnr.it (A.D.); mcalamante@iccom.cnr.it (M.C.); gianna.reginato@iccom.cnr.it (G.R.)
* Correspondence: adalgisa.sinicropi@unisi.it

Received: 13 March 2020; Accepted: 16 April 2020; Published: 19 April 2020

Abstract: The prediction of ground-state redox potentials by quantum chemical methods has a prominent role in the rational design of novel organic photosensitizers both for dye-sensitized solar cells (DSSCs) and photocatalytic systems for the production of H_2. Indeed, the ground-state redox potential of the photosensitizers is one of the key parameters to identify the most promising candidates for such applications. Here, the ground-state redox potentials of 16 organic donor-π-acceptor D-π-A and donor-acceptor-π-acceptor D-A-π-A dyes having a medium to large size of the conjugated scaffold are evaluated, using the methods of the Density Functional Theory (DFT), in terms of free energy differences between their neutral and oxidized ground-state forms. These results are compared to the available experimental data and to the computed highest occupied molecular orbital energy $-\varepsilon$(HOMO) values as an approximation of ground-state redox potentials according to Koopmans' theorem. Using the MPW1K functional in combination with the 6-31+G* basis set, the strategy based on the free energy cycle, including solvent effects, reproduces with a good level of accuracy the observed values (mean absolute error (MAE) < 0.2 eV) and trend of redox potentials within related families of dyes. On the other hand, the $-\varepsilon$(HOMO) values are only able to capture the experimental trends in redox potential values.

Keywords: dye-sensitized solar cells; first principle modelling; ground-state oxidation potentials; solar energy devices; solar fuel devices; organic sensitizers; photocatalytic hydrogen production

1. Introduction

Organic dyes having a donor-π-acceptor (D-π-A) or donor-acceptor-π-acceptor (D-A-π-A) architecture have been extensively used as photosensitizers in dye-sensitized solar cells (DSSCs) [1–3] and, more recently, as sensitizers in photocatalytic systems for the production of H_2 [4–7]. In both devices, visible-light absorbing dyes are employed to enhance light harvesting of semiconductor nanoparticles of TiO_2.

The use of synthetic organic push-pull dyes is becoming increasingly popular [6]. In particular, donor–acceptor D-π-A architectures, have been found able to establish an efficient charge separation: indeed, due to the wide diversity of suitable D, A and π fragments a huge number of different sensitizers can be accessed, allowing a fine-tuning of their chemical, optical, energetic, and stability properties. In addition, recently, the use of sensitizers based on the D−A−π−A architecture has been investigated, finding that the additional acceptor is useful for modulating the energy levels, extending the light harvesting ability, as well as improving photovoltaic performances and photostability. Indeed, the additional electron acceptor unit can enhance the intramolecular electronic push−pull effect, thus significantly affecting the energy levels and absorption properties of sensitizers [8].

In DSSCs, the dye absorbs light and, upon excitation, it transfers an electron to the conduction band of the semiconductor, which carries it to a glass electrode (transparent conducting oxide layer); at the same time, the resulting hole is transferred from the dye/sensitizer to the redox mediator (usually an I^-/I_3^- redox couple) which, through an oxidation-reduction interchange, carries it to the counter-electrode, thereby closing the circuit and generating a current (See Figure 1a).

The photocatalytic systems, on the other hand, are dye-sensitized Pt/TiO_2 photocatalysts in which the dye, as in DSSCs, harvests visible light and injects the electron in the TiO_2 conduction band (See Figure 1b). Electrons are then transferred to Pt^0 nanoparticles, which are adsorbed on the TiO_2 surface and here protons are reduced to H_2. The regeneration of the oxidized dye occurs by using a sacrificial electron donor (SED) agent. Triethanolamine (TEOA), ethylenediaminetetraacetic acid (EDTA), ascorbic acid (AA) and, more recently, ethanol, have been employed as SEDs [4].

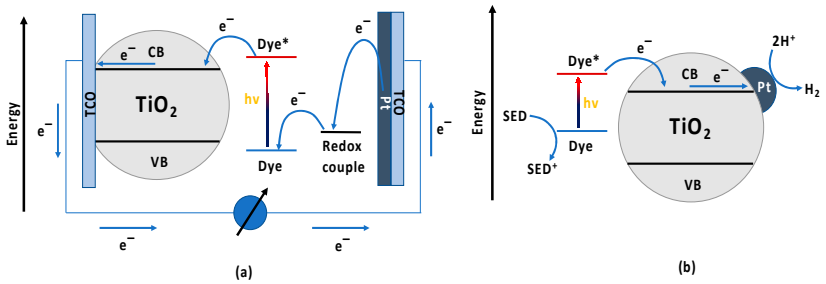

Figure 1. Energy levels and working mechanisms of: (**a**) dye-sensitized solar cells and (**b**) dye-sensitized Pt/TiO_2 photocatalysts.

Among other requirements, the correct alignment of the relative energy levels of the dye and the redox couple in DSSCs or the SED in the Pt/TiO_2 photocatalysts is a key issue that affects the overall efficiency of both dye-sensitized systems. Indeed, the effective regeneration of the oxidized dye is pivotal for both devices to obtain good performances in terms of efficiency. Thus, a key parameter for an efficient dye to be employed is the ground-state redox potential (GSRP) since this value, especially when compared to the redox couple or SED energy levels, is a measure of the dye regeneration driving force.

The prediction of GSRP by quantum chemical methods is of outstanding importance for the rational design of novel organic sensitizers and greatly contributes to the development of more efficient devices. Indeed, the calculations of these photoelectrochemical properties along with the modeling of other key parameters such as the excited state redox potential, the vertical excitation and emission energies, the charge transfer nature of the excitation process and the electronic coupling between the dye and the semiconductor, would indicate the most promising dye candidates for solar energy and fuel (H_2) devices. This strategy has been intensely applied in literature for the molecular engineering of the organic sensitizer for DSSC [9–14], mostly using the methods of the density functional theory (DFT) and its time-dependent extension (TDDFT).

The accurate evaluation of GSRP is hard to achieve, especially because it has been shown that the accuracy deteriorates as the conjugation length of the molecule increases [15]. In the present study,

the GSRP of 16 organic dyes having a medium to large conjugation length (see molecules in Figure 2) have been computed using DFT, and in particular the MPW1K functional [16,17], which has been shown to give the best accuracy before [15], and a polarizable continuum model (PCM) [18] to take into account solvent effects. To the best of our knowledge, this is the first work dealing with the calculations of GSRP of a relatively large set of organic dyes having a medium to large size of the conjugated scaffold. The DFT predicted values had been compared to the available experimental data showing that the employed strategy allows reproducing the GSRP with a mean absolute error <0.2 eV.

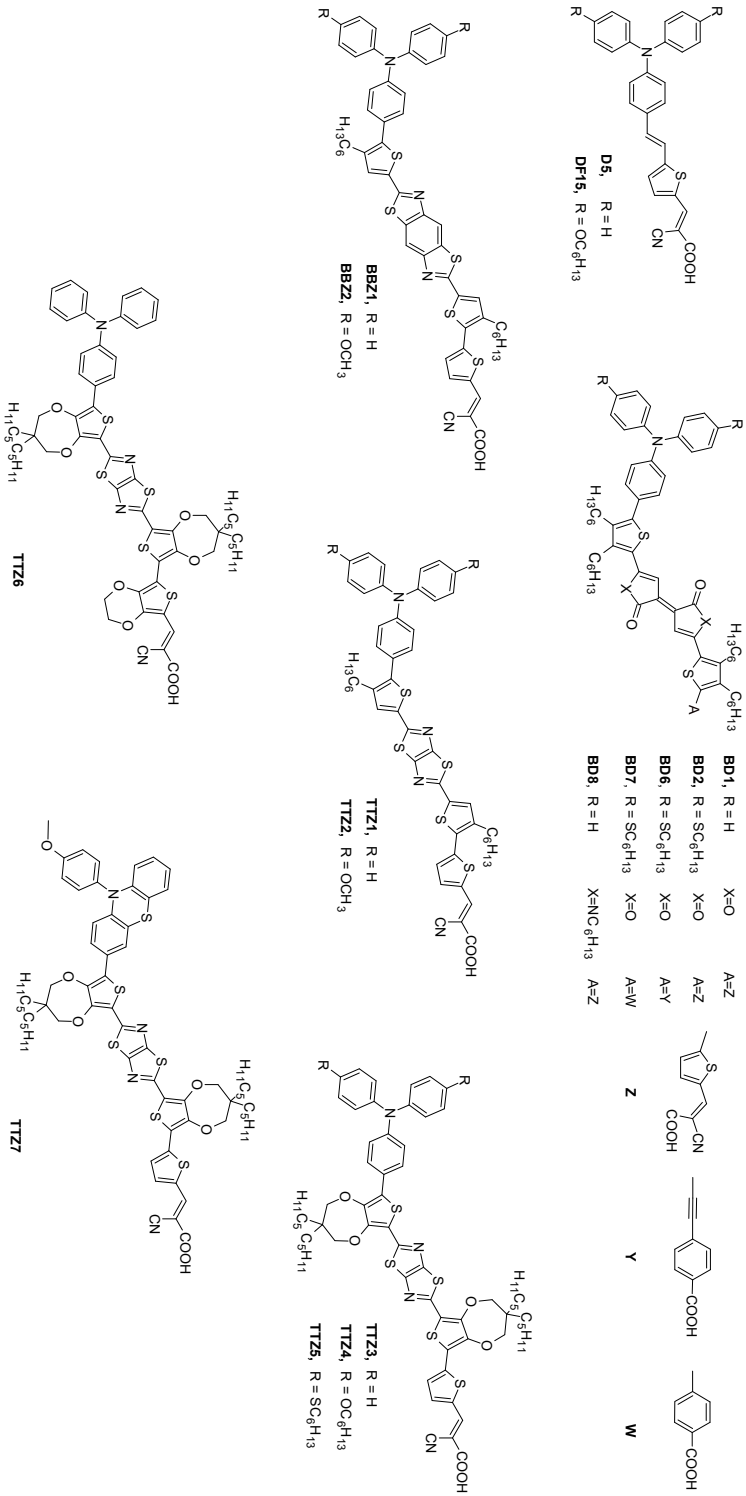

Figure 2. Investigated set of molecules.

2. Methods

All quantum mechanical(QM) calculations were performed using density functional theory (DFT) and time-dependent DFT (TDDFT) [19] using the G09 program package [20]. The ground-state redox potential was computed at the MPW1K/6-31+G* level of theory as free energy differences between the neutral and oxidized state of these dyes following the procedure described by Pastore et al. [15].

More specifically, $GSRP = \left(G^0 - G^+\right)solv$ where both G^0_{solv} and G^+_{solv} are obtained by adding the solvent effect to the free energies of the gas-phase optimized molecules: $G^0_{solv} = G^0_{vac} + \Delta G^0_{solv}$ and $G^+_{solv} = G^+_{vac} + \Delta G^+_{solv}$. G^0_{vac} and G^+_{vac} are obtained by performing a single point calculation at the optimized geometry in vacuo, followed by frequency calculations. The free energies of solvation ΔG^0_{solv} and ΔG^+_{solv} are estimated as the free energy difference between the system in solution and in gas-phase, calculated at the geometry optimized in solution.

Neutral and oxidized ground-state geometries of all dyes were computed using the MPW1K [16,17] functional in combination with 6-31G* and 6-31+G* basis set both in gas-phase and in the presence of dichloromethane (DCM) as a solvent. The MPW1K functional choice was made as it was shown to be the method providing results closer to the experimental values when used for the calculations of GSRPs in smaller but related D-π-A dyes [15]. Solvent effects were added via PCM [18]. DCM is the solvent experimentally employed for the electrochemical measurements. Indeed, a rigorous way to obtain the ground state redox potential needs to consider in the calculation energy terms including geometry relaxation energy connected with changes of electronic structure and changes of the solvation energies.

Initial structures for the ground-state geometry optimization were built starting from their B3LYP/6-31G* optimized geometries, for which the most stable among the possible conformers had been identified in our previous papers (see References [10,12,21–23]).

DFT frontier molecular orbitals and spin densities of the cation species were computed at MPW1K/6-31+G* level both in vacuo and using PCM.

Minus the value of the highest occupied molecular orbital (HOMO) energies, -ε(HOMO), were evaluated both in gas-phase and in DCM, for the neutral state of all dyes at their optimized geometry in DCM.

Vertical excitation energies (E_{exc}), absorption maxima (λ_{max}), and oscillator strengths (f) were computed at the time-dependent DFT (MPW1K/6-31+G*) level on all the optimized structures. Again, the PCM was used to include the effect of the solvent. These results are shown in the Supplementary Materials.

Electrochemical experiments were conducted on N_2-saturated solutions of the compound under study in freshly distilled dichloromethane, in the presence of electrochemical grade [Bu_4N] [PF_6] (0.1 M) as supporting electrolyte (Merck). Cyclic voltammetry was performed in a three-electrode cell using a glassy carbon working electrode, a platinum counter electrode, and an AgCl/Ag (NaCl 3 M) reference electrode. A Bioanalytical Systems (BAS) 100 W electrochemical analyzer was used as polarizing unit. $E_{S+/S}$ values were obtained as standard potentials by averaging the values of the anodic and cathodic peaks and using the ferrocenium/ferrocene couple as an external standard. All the potential values were then referred to normal hydrogen electrode (NHE) by using a value of +0.63 V for ferrocene *vs.* NHE [24]. Typical analyte concentration was approx. 10^{-3} M.

3. Results and Discussion

All the investigated dyes (see Figure 2) were based on fully conjugated D-π-A or D-A-π-A structures, the latter having an auxiliary acceptor group in the central part of the molecule. D5 and DF15 were triarylamine-thiophene derivatives bearing cyanoacrylic acid as anchoring group. The heterocyclic benzobisthiazole- and thiazolothiazole-systems constituted the central π scaffold of BBZ1,2 and TTZ1-7 sensitizers, respectively. The last group of molecules (BD1,2,6,7,8) contained an electron-poor *bis*-lactone moiety (Pechmann lactone) connected to thiophenes decorated with various donor and acceptor groups. With the only exception of compound D5 [25], the investigated dyes were selected based on reliable experimental data available, having been designed, characterized and synthetized in our laboratories, as described in our previous works [4,10,21–23].

The neutral ground-state geometries of these dyes, computed at the MPW1K/6-31+G* level, are shown in Figure S1 (see Supplementary Materials). All the dyes assumed a largely planar structure along most of the conjugated system with a deviation from coplanarity (ranging from 27° to 49°) between the triarylamine and the linked thiophene. To assess the quality of the MPW1K/6-31+G* optimized structures, their vertical excitation energies were computed at the TDDFT level and the comparison between these results and experimental values is shown in Table S1 of the Supplementary Materials. The mean absolute error was about 0.06 eV, which clearly indicates the accuracy of the optimized structures and the high degree of accuracy of MPW1K functional in dealing with the excited states of the analyzed D-π-A or D-A-π-A dyes. Table S1 (see Supplementary Materials) also shows that the main electronic transition was, in all cases, a HOMO→LUMO transition with a smaller contribution of a HOMO−1→LUMO transition. From the plot of the corresponding DFT frontier molecular orbitals collected in Table S2 of the Supplementary Materials, it is clear that the HOMO and LUMO were mostly localized on the donor and acceptor unit, respectively, albeit still with a sizable contribution of the conjugated scaffold.

Given the good performance of the MPW1K functional in reproducing the vertical excitation energies (this work) and in computing excited state geometries and vertical emission energies [12], the choice of MPW1K functional appears appropriate also to compute GSRP. Additionally, in a previous paper, the MPW1K has been demonstrated to be by far the method that provided computed GSRP values closer to the experimental ones [15].

The results of GSRP computed *vs* experimental $E_S{}^{+}{}_{/S}$ values on all the investigated dyes are shown in Figure 3. The graph is built from raw data of Table S3 ($GSRP^{b\text{-}d}$). The analysis of the computed values leads to some interesting considerations. At first glance, it is straightforward to observe that data covered two distinct regions of the graph: GSRP values calculated in the gas-phase overestimated the experimental value (black circles in the region above the diagonal, where $y = x$, i.e., calculated (y) = experimental (x)), while GSRP values calculated in the presence of the solvent slightly underestimated the experimental value (red and blue circles, below the diagonal). The use of high-quality basis sets in the geometry calculation visibly improved the agreement between the calculated GSRP and experimental potential values (red circles). From the quantitative point of view, the highest level of theory employed, i.e., computing frequencies at the MPW1K/6-31+G* on neutral and oxidized state geometries optimized at the same level (MPW1K/6-31+G*//MPW1K/6-31+G*) was the one that provided the most accurate values with a mean absolute error (MAE) of 0.18 eV (red circles). Higher deviations from experiments were found applying the MPW1K/6-31+G* combination on neutral and oxidized state geometries computed at the MPW1K/6-31G* level (MPW1K/6-31+G*//MPW1K/6-31G*). Indeed, the MAE was about 0.32 eV (blue circles). The highest deviations from experiments were provided by the GSRP calculations in terms of free energies using the MPW1K/6-31+G*//MPW1K/6-31+G* level in gas-phase (black circles). Thus, we may conclude that the difference of the free energy values allows, at least, to correctly reproduce the redox potential qualitative trend, while calculations using the use of the MPW1K/6-31+G*//MPW1K/6-31+G* level in the presence of the solvent is crucial to correctly reproduce the quantitative trend.

According to Koopmans' theorem [26], related to the closed-shell Hartree-Fock theory and extended to Kohn-Sham orbital energies within the DFT [27,28], the negative of the HOMO energy is equal to the first ionization energy of a system, which is the minimum energy required to remove an electron from the HOMO of a molecule. The first ionization energy of a system can be related to the energy involved in the oxidation (loss of electrons) of a molecule and therefore to $E_{S+/S}$.

Thus, -ε(HOMO) values were also computed both in gas-phase (Figure 3, grey triangles and Figure 5, blue circles) and in DCM (Figure 3, grey asterisks and Figure 5, brown circles)) giving a MAE of 0.50 and 0.56 eV, respectively. The data provided by the computation of -ε(HOMO) values in gas-phase were slightly closer to the experimental values than the -ε(HOMO) values computed in solution. This evidence could be related to the fact that, for the investigated molecules in the gas-phase, the orbitals of the charged and neutral species are nearly identical and orbital relaxation is not expected.

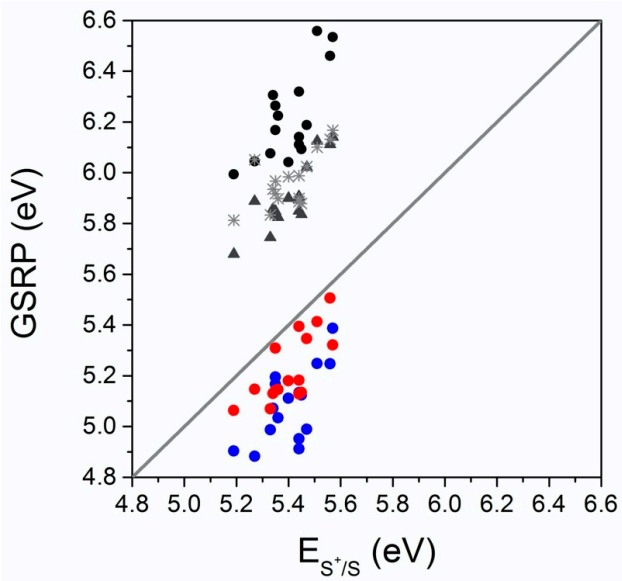

Figure 3. Computed ground state redox potential (GSRP) values ($GSRP^{b\text{-}d}$ in Table S3) vs. experimental $E_{S^+/S}$ values. The $y = x$ diagonal is reported as a reference. Black circles: MPW1K/6-31+G*//MPW1K/6-31+G* values in gas-phase; blue circles: MPW1K/6-31+G*//MPW1K/6-31G* values in DCM; red circles MPW1K/6-31+G*//MPW1K/6-31+G* values in dichloromethane (DCM); grey triangles: minus the value of the highest occupied molecular orbital energies, $-\varepsilon$(HOMO) in gas-phase; grey asterisks: $-\varepsilon$(HOMO) in DCM.

Since the difference $\Delta\varepsilon = \varepsilon\ (\mathrm{HOMO})_{\mathrm{vac}} - \varepsilon(\mathrm{HOMO})_{\mathrm{solv}}$ broadly varies from ~ 0 to a few hundreds of meV, we further investigated three of the dyes, namely TTZ7 (a large molecule with the largest $\Delta\varepsilon$), BD2 (a large molecule with $\Delta\varepsilon \approx 0$) and D5 (a small molecule with $\Delta\varepsilon \approx 0$). To probe the extent of the orbital relaxation, the HOMO of each neutral dye was compared with the spin-density surface calculated for its cation; orbital relaxation should produce visible differences in the space localization of these two surfaces. Figure 4 shows how, for D5 and BD2, the HOMO of the neutral dye and the spin density of its cation had a very similar shape and space distribution, both in the gas-phase and in DCM. Therefore, in this case, the orbital relaxation was minimal and Koopmans' theorem was expected to be valid, either in gas phase or in solution. On the other hand, the HOMO of TTZ7 and the spin density of $TTZ7^+$ had a similar shape and space distribution in the gas-phase. In contrast, in solution, the spin density was much more localized on the donor region as an effect of the orbital rearrangement. Localization of the charge on a more restricted region was possible because of the stabilizing interaction with the solvent. In this case, there were not favorable conditions to apply Koopmans' theorem. In general, charge localization is driven by the presence of electron-withdrawing groups, facilitated by the larger size of the molecule and made possible by the presence of the solvent. At the same time, charge delocalization is favored by the relief of the interelectronic repulsion and made possible by the presence of an efficient conjugation path. Considering all these aspects, after having analyzed the conformation, the dimensions and the presence of electron-withdrawing groups, it has not been possible to univocally identify the reason why a more marked charge localization is observed only in some cases. Reasonably this interesting aspect will require a dedicated study and may be the subject of subsequent work, but we will have to settle for this further caveat against the uncritical use of Koopmans' theorem.

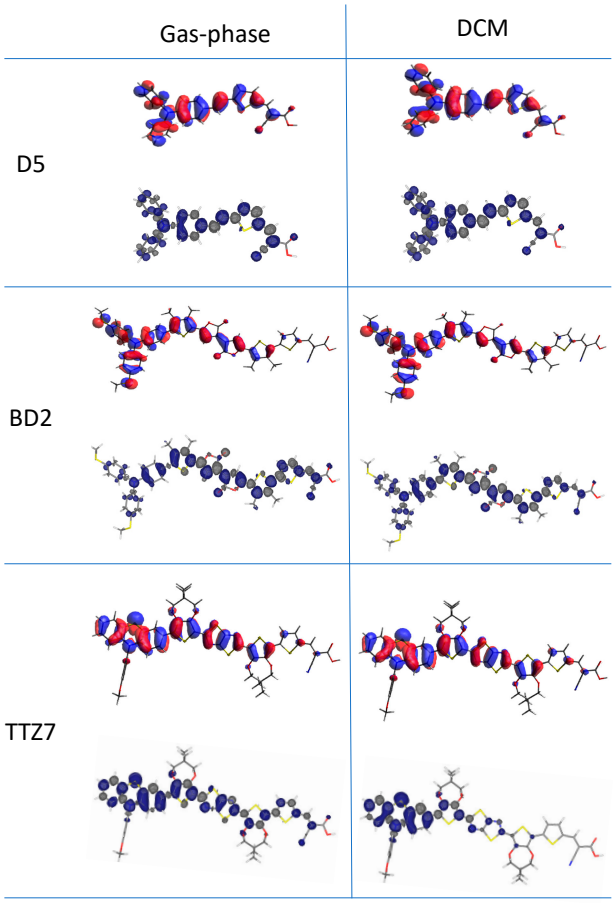

Figure 4. HOMO of the neutral species (top) and the spin density of its cation (bottom) in gas-phase (left) and DCM (right) for D5, BD2 and TTZ7 dyes computed at the MPW1K/6-31+G* level and plotted using Avogadro [29,30] and Chemcraft [31] softwares, respectively.

Inspection of Figure 5, which collects the computed GSRP vs. dyes, reveals that, considering closely related compounds with similar scaffolds, computed GSRPs and -ε(HOMO) reproduced the same trends found for the experimental values. For example, GSRP and -ε(HOMO) values of DF15 were lower in energy than those of D5, due to the presence of a stronger hexyloxy-substituted donor group in DF15. Both dyes had more positive values than the redox potential of the conventionally and commonly used redox couple in DSSC, i.e., the iodide/triiodide redox couple (4.77 eV) [32], as well some Co-based redox systems (4.85–5.04 eV) [33] suggesting that regeneration of the sensitizer is feasible. Similar considerations apply to the Pechmann lactone containing molecules (BD1,2,6,7,8) and to the benzobisthiazole- (BBZ1,2) and thiazolothiazole-systems (TTZ1-7). In particular, and again in agreement with the experimental values, the introduction of a stronger donor group in BD2 compared to the one present in BD1, and the substitution of the lactone moiety of BD1 with the less electron-withdrawing lactam in BD8, determined the lowering of the GSRP. Moreover, the substitution of the cyanoacrylic acid with a less electron-withdrawing acceptor (BD6 and BD7 vs. BD2) provided experimental ground-state oxidation potentials similar to BD2. While the computed GSRP and -ε(HOMO) values for BD6 and -ε(HOMO) value for BD7 are in line with this observation, GSRPs of BD7 were instead predicted to be higher in energy although closer to the experimental values. Concerning the benzobisthiazole- (BBZ1,2) and thiazolothiazole-systems (TTZ1-7), the introduction of electron-rich methoxy-substituents on TTZ2 and BBZ2 led to a decrease in the ground-state oxidation potentials compared to TTZ1 and BBZ1, respectively, which is also evident in the computational results. In the series TTZ3-7, in line with experiments, the introduction of the electron-donating alkoxy groups on the triarylamine portion in TTZ4 and the presence of the terminal phenothiazine unit in TTZ7

resulted in lowering ground-state oxidation potential values. However, all BBZs and TTZs dyes had ground-state oxidation potentials more positive than that of the iodide/triiodide couple, thus assuring dye regeneration. The present results are consistent with the following final observations: (i) the frontier orbital approximations, according to Koopmans' theorem, might be used to reproduce the trend of standard potentials in closely related families of compounds but cannot be used as a method to predict quantitative values; (ii) to obtain GSRPs with a certain degree of accuracy sufficient to be comparable with experimental standard potentials, free energy differences computations including solvent effects need to be taken into account.

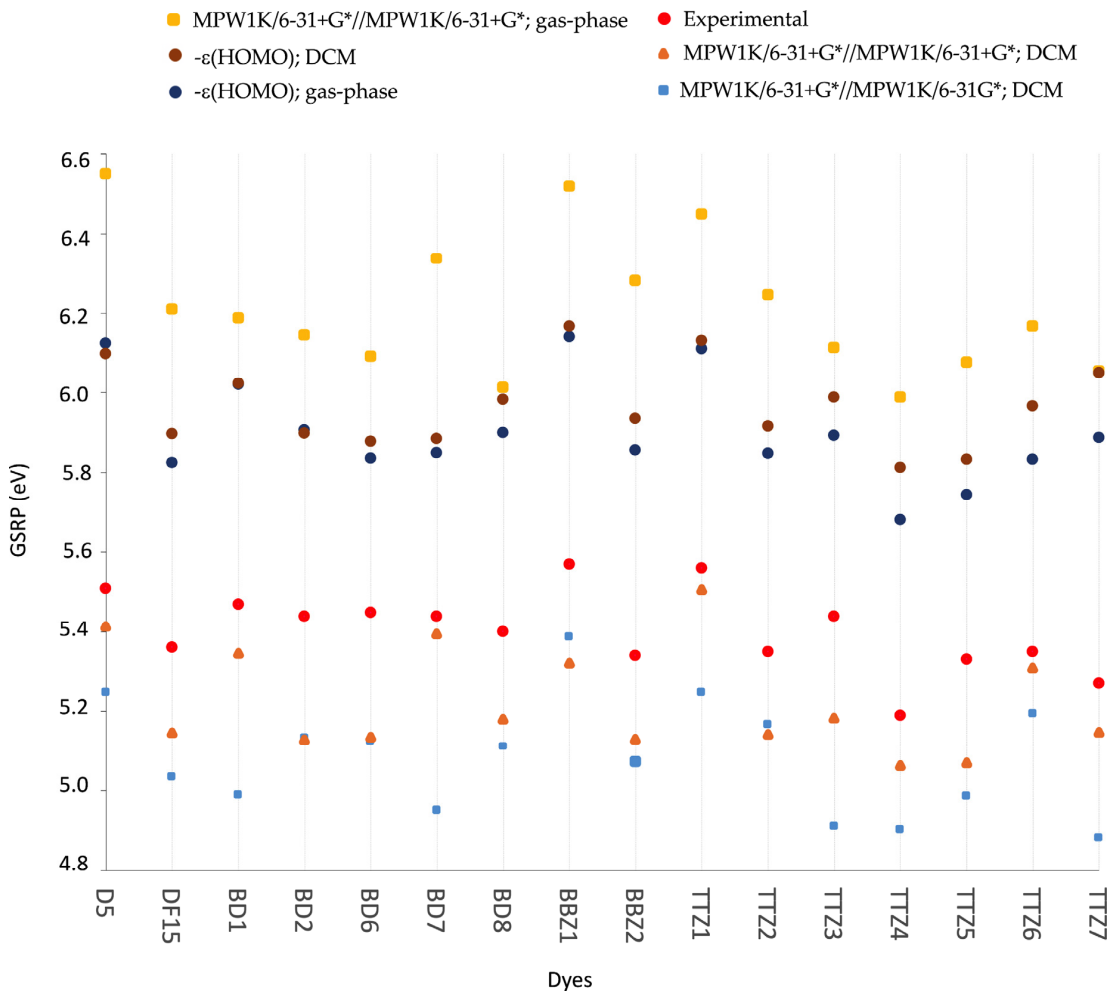

Figure 5. Experimental, computed GSRP and $-\varepsilon$(HOMO) of dye sensitizers.

4. Conclusions

The present study shows that, using the MPW1K functional in combination with an appropriate basis set, the prediction of GSRP of a relatively large set of D-π-A/D-A-π-A dyes having a medium to large size of the conjugated scaffold can be obtained with a good level of accuracy. Moreover, the experimental trends in GSRP values of closely related compounds with similar scaffolds are well reproduced. Thus, the employed strategy should help researchers to identify sensitizers that can efficiently be used in DSSCs or in photocatalytic systems for the production of H_2, allowing them to concentrate precious time and resources only on the preparation of the most promising candidates.

Supplementary Materials: The following are available online at http://www.mdpi.com/1996-1073/13/8/2032/s1, Table S1: TDDFT (MPW1K/6-31+G*//MPW1K/6-31+G*) absorption maxima ($\lambda^a{}_{max}$ (nm)), excitation energies (E_{exc} (eV)), oscillator strenghts (f) and transition contributions (%). Solvent effects are included via PCM. The same solvents used in the experiments have been modeled. The experimental $\lambda^a{}_{max}$ and corresponding E_{exc} are

given in brackets. Table S2: DFT frontier molecular orbitals for all dyes obtained at MPW1K/6-31 + G* level in vacuo. Table S3: Experimental ($E_{S+/S}$), computed GSRP (eV) and - ε(HOMO) of all investigated dyes. Cartesian Coordinated of all the investigated dyes in gas-phase and in solvent, Figure S1. MPW1K/6-31+G* optimized geometries of all dyes computed in vacuo and in DCM (in brackets). Dihedral angles are given in degrees.

Author Contributions: Conceptualization, F.F.d.B. and A.S.; investigation, S.M., C.C., M.L.P., and A.S.; writing—original draft, S.M., F.F.d.B., and A.S.; writing—review and editing, S.M., F.F.d.B., C.C., M.L.P, L.Z., A.D., M.C., G.R., R.B., and A.S.; funding acquisition, R.B. and A.S. All authors have read and agreed to the published version of the manuscript.

Funding: This research received no external funding.

Acknowledgments: S.M.: F.F, C.C., M.L.P., R.B., and A.S acknowledge MIUR Grant—Department of Excellence 2018-2022. S.M. is grateful for the Ph.D. grant within the "Progetto Pegaso" funded by Regione Toscana.

Conflicts of Interest: The authors declare no conflict of interest.

References

1. Hagfeldt, A.; Boschloo, G.; Sun, L.; Kloo, L.; Pettersson, H. Dye-Sensitized Solar Cells. *Chem. Rev.* **2013**, *110*, 159–184.
2. Lee, C.P.; Li, C.T.; Ho, K.C. Use of organic materials in dye-sensitized solar cells. *Mater. Today* **2017**, *20*, 267–283. [CrossRef]
3. Gong, J.; Sumathy, K.; Qiao, Q.; Zhou, Z. Review on dye-sensitized solar cells (DSSCs): Advanced techniques and research trends. *Renew. Sustain. Energy Rev.* **2017**, *68*, 234–246. [CrossRef]
4. Dessì, A.; Monai, M.; Bessi, M.; Montini, T.; Calamante, M.; Mordini, A.; Reginato, G.; Trono, C.; Fornasiero, P.; Zani, L. Towards Sustainable H2 Production: Rational Design of Hydrophobic Triphenylamine-based Dyes for Sensitized Ethanol Photoreforming. *ChemSusChem* **2018**, *11*, 793–805. [CrossRef] [PubMed]
5. Zhang, X.; Peng, T.; Shuaishuai, S. Recent advances in dye-sensitized semiconductor systems for photocatalytic hydrogen production. *J. Mater. Chem. A Mater. Energy Sustain.* **2016**, *4*, 2365–2402. [CrossRef]
6. Cecconi, B.; Manfredi, N.; Montini, T.; Fornasiero, P.; Abbotto, A. Dye-Sensitized Solar Hydrogen Production: The Emerging Role of Metal-Free Organic Sensitizers. *Eur. J. Org. Chem.* **2016**, *2016*, 5194–5215. [CrossRef]
7. Watanabe, M. Dye-sensitized photocatalyst for effective water splitting catalyst. *Sci. Technol. Adv. Mater.* **2017**, *18*, 705–723. [CrossRef]
8. Wu, Y.; Zhu, W.H.; Zakeeruddin, S.M.; Grätzel, M. Insight into D−A−π−A Structured Sensitizers: A Promising Route to Highly Efficient and Stable Dye-Sensitized Solar Cells. *ACS Appl. Mater. Interfaces* **2015**, *7*, 9307–9318. [CrossRef]
9. De Angelis, F.; Fantacci, S.; Selloni, A. Alignment of the dye's molecular levels with the TiO2band edges in dye-sensitized solar cells: A DFT-TDDFT study. *Nanotechnology* **2008**, *19*, 15–17. [CrossRef]
10. Dessì, A.; Calamante, M.; Mordini, A.; Peruzzini, M.; Sinicropi, A.; Basosi, R.; Fabrizi de Biani, F.; Taddei, M.; Colonna, D.; Di Carlo, A.; et al. Organic dyes with intense light absorption especially suitable for application in thin-layer. *Chem. Commun.* **2014**, *50*, 13952–13955. [CrossRef]
11. Pastore, M.; Fantacci, S.; De Angelis, F. Modeling Excited States and Alignment of Energy Levels in Dye-Sensitized Solar Cells: Successes, Failures, and Challenges. *J. Phys. Chem. C* **2013**, *117*, 3685–3700. [CrossRef]
12. Bernini, C.; Zani, L.; Calamante, M.; Reginato, G.; Mordini, A.; Taddei, M.; Basosi, R.; Sinicropi, A. Excited state geometries and vertical emission energies of solvated dyes for DSSC: A PCM/TD-DFT benchmark study. *J. Chem. Theory Comput.* **2014**, *10*, 3925–3933. [CrossRef]
13. Fantacci, S.; De Angelis, F. Ab Initio Modeling of Solar Cell Dye Sensitizers: The Hunt for Red Photons Continues. *Eur. J. Inorg. Chem.* **2019**, *2019*, 743–750. [CrossRef]
14. Chiu, C.C.; Sheng, Y.C.; Lin, W.J.; Juwita, R.; Tan, C.J.; Gavin Tsai, H.H. Effects of internal electron-withdrawing moieties in d−a−π−a organic sensitizers on photophysical properties for DSSCs: A computational study. *ACS Omega* **2018**, *3*, 433–445. [CrossRef] [PubMed]
15. Pastore, M.; Fantacci, S.; De Angelis, F. Ab Initio Determination of Ground and Excited State Oxidation Potentials of Organic Chromophores for Dye-Sensitized Solar Cells. *J. Phys. Chem. C* **2010**, 22742–22750. [CrossRef]
16. Lynch, B.J.; Fast, P.L.; Harris, M.; Truhlar, D.G. Adiabatic Connection for Kinetics. *J. Phys. Chem. A* **2000**, *104*, 4811–4815. [CrossRef]

17. Zhao, J.; Lynch, B.J.; Truhlar, D.G. Development and Assessment of a New Hybrid Density Functional Model for Thermochemical Kinetics. *J. Phys. Chem. A* **2004**, *108*, 2715–2719. [CrossRef]
18. Tomasi, J.; Mennucci, B.; Cammi, R. Quantum Mechanical Continuum Solvation Models. *Chem. Rev.* **2005**, *105*, 2999–3094. [CrossRef]
19. Lecture Notes in Physics. In *Fundamentals of Time-Dependent Density Functional Theory*; Marques, M.A.L.; Maitra, N.T.; Nogueira, F.M.S.; Gross, E.K.U.; Rubio, A. (Eds.) Springer: Berlin/Heidelberg, Germany, 2012; Volume 837, ISBN 978-3-642-23517-7.
20. Frisch, M.J.; Trucks, G.W.; Schlegel, H.B.; Scuseria, G.E.; Robb, M.A.; Cheeseman, J.R.; Scalmani, G.; Barone, V.; Mennucci, B.; Petersson, G.A.; et al. *Gaussian 09, Revision C.01*; Gaussian, Inc.: Wallingford, CT, USA, 2010.
21. Dessì, A.; Calamante, M.; Mordini, A.; Peruzzini, M.; Sinicropi, A.; Basosi, R.; De Biani, F.F.; Taddei, M.; Colonna, D.; Di Carlo, A.; et al. Thiazolo[5,4-d]thiazole-based organic sensitizers with strong visible light absorption for transparent, efficient and stable dye-sensitized solar cells. *RSC Adv.* **2015**, *5*, 32657–32668. [CrossRef]
22. Dessì, A.; Consiglio, B.; Calamante, M.; Reginato, G.; Mordini, A.; Peruzzini, M.; Taddei, M.; Sinicropi, A.; Parisi, L.; de Biani, F.F.; et al. Organic Chromophores Based on a Fused Bis-Thiazole Core and Their Application in Dye-Sensitized Solar Cells. *Eur. J. Org. Chem.* **2013**, *2013*, 1916–1928. [CrossRef]
23. Dessì, A.; Sinicropi, A.; Mohammadpourasl, S.; Basosi, R.; Taddei, M.; de Biani, F.F.; Calamante, M.; Zani, L.; Mordini, A.; Bracq, P.; et al. New Blue Donor—Acceptor Pechmann Dyes: Synthesis, Spectroscopic, Electrochemical, and Computational Studies. *ACS Omega* **2019**, *4*, 7614–7627. [CrossRef] [PubMed]
24. Pavlishchuk, V.V.; Addison, A.W. Conversion constants for redox potentials measured versus different reference electrodes in acetonitrile solutions at 25 °C. *Inorg. Chim. Acta* **2000**, *298*, 97–102. [CrossRef]
25. Hagberg, D.P.; Edvinsson, T.; Marinado, T.; Boschloo, G.; Hagfeldt, A.; Sun, L. A novel organic chromophore for dye-sensitized nanostructured solar cells. *Chem. Commun.* **2006**, *21*, 2245–2247. [CrossRef] [PubMed]
26. Koopmans, T. Über die Zuordnung von Wellenfunktionen und Eigenwerten zu den einzelnen Elektronen eines Atoms. *Physica* **1934**, *1*, 104–113. [CrossRef]
27. Koopmans, T. Proof that $\frac{\partial E}{\partial n_i} = \varepsilon$ in density-functional theory. *Phys. Rev. B* **1978**, *18*, 7165. [CrossRef]
28. Conradie, J. A Frontier orbital energy approach to redox potentials. *J. Phys. Conf. Ser.* **2015**, *633*, 012045. [CrossRef]
29. Hanwell, M.D.; Curtis, D.E.; Lonie, D.C.; Vandermeersch, T.; Zurek, E.; Hutchison, G.R. Avogadro: An advanced semantic chemical editor, visualization, and analysis platform. *J. Cheminform.* **2012**, *4*, 17. [CrossRef] [PubMed]
30. Avogadro: An Open-Source Molecular Builder and Visualization Tool. Version 1.1.1. Available online: http://avogadro.cc/ (accessed on 19 April 2020).
31. Chemcraft—Graphical Software for Visualization of Quantum Chemistry Computations. Available online: https://www.chemcraftprog.comtle (accessed on 19 April 2020).
32. Boschloo, G.; Hagfeldt, A. Characteristics of the Iodide/Triiodide Redox Mediator in Dye-Sensitized Solar Cells. *Acc. Chem. Res.* **2009**, *42*, 1819–1826. [CrossRef] [PubMed]
33. Feldt, S.M.; Gibson, E.A.; Gabrielsson, E.; Sun, L. Design of Organic Dyes and Cobalt Polypyridine Redox Mediators for High-Efficiency Dye-Sensitized Solar Cells. *J. Am. Chem. Soc.* **2010**, *132*, 16714–16724. [CrossRef] [PubMed]

© 2020 by the authors. Licensee MDPI, Basel, Switzerland. This article is an open access article distributed under the terms and conditions of the Creative Commons Attribution (CC BY) license (http://creativecommons.org/licenses/by/4.0/).